Tunable time delay in active fiber Bragg grating coupler*

LI Qi-liang(李齐良)**, **WANG Zi-yang**(王紫阳), **ZHANG Yong**(张勇), **WANG Tian-shu**(王天枢), **ZENG Ran**(曾然), **and HU Miao**(胡淼)

Institute of Communication and Information, College of Communication Engineering, Hangzhou Dianzi University, Hangzhou 310018, China

(Received 12 July 2012)

Slowing down velocity and controlling time delay of optical pulses in fiber have many potential applications in optical communication systems, and a number of theoretical and experimental studies have been done. In this paper, the transmission spectrum and reflective spectrum of active fiber Bragg grating (FBG) couplers are studied, and the analytic expressions of dispersion and time delay are obtained. By changing the detuning and gain coefficient, different dispersions and time delays in active fiber Bragg grating coupler are obtained. The results show that different detunings and gain coefficients can result in various time delays, and thus tunable time delay could be achieved by changing signal frequency or gain coefficient.

Document code: A **Article ID:** 1673-1905(2012)06-0433-4

DOI 10.1007/s11801-012-2307-5

Fiber Bragg gratings (FBGs) have many applications in the optical communications system, such as optical filters, optical amplifiers and dispersion compensators[1-3]. The combination of Bragg gratings with fiber couplers will form fiber Bragg grating couplers (FBGCs). Active FBGCs can be executed by doping rare-earth elements in ordinary FBGCs, which can meet the requirement of high operation power[4].

Tunable time delay of optical pulses in fiber has many potential applications in optical communication systems, such as optical buffer, signal processing, data synchronization and all-optical router[5,6]. The issues of group delay and group velocity control of FBGs have received increasing interest in the recent years, and a number of schemes have been studied and experimentally demonstrated[7-13], such as group delay in Bragg grating with linear chirp[8], dispersionless slow light using gap solitons[10] and group delay in active FBG[9,11-13]. The group delay generated by the active FBG refiection can be tuned by optically pumping the active FBG with different pumping power[12]. A gain-controlled transition of pulse reflection from superluminal light to subluminal light is analytically investigated with a π phase shift in uniform gratings and tapered gratings[11]. Qian[9] proposed and experimentally demonstrated a slow-light technique to tune optical delay by using the Er/Yb co-doped FBG. H. Shahoei[12] proposed and demonstrated tunable time delay of FBGs written in Er/Yb co-doped fiber, and a continuously tunable time delay up to 200 ps for a Gaussian pulse of 7.6 GHz was experimentally demonstrated by using a linearly chirped FBG (LCFBG). The group delay responses of the LCFBG pumped by the 980 nm laser diode at different pumping power in an unbalanced temporal pulse shaping system were studied[13].

In this paper, we propose a scheme to control time delay by changing the pump power in an active FBGC. The FBGC, which is an FBG with the excellent wavelength selection property and a fiber coupler with multi-port property, is suitable for add-drop multiplexing.

We only consider symmetric FBGC, in which the two cores have the same parameters. Using Maxwell electromagnetic theory, coupled-mode equations in active FBGC can be obtained. Considering the simplest case that a low-power continuous wave (CW) beam is incident on one of the input ports of an FBGC, the time-dependent terms can be set to zero. Since the nonlinear terms are also negligible, the coupled-mode equations become

$$\begin{cases} \mathrm{i}\dfrac{\partial u_1}{\partial z}+(\delta-\mathrm{i}\,g)u_1+\kappa v_1+Cu_2=0 \\ -\mathrm{i}\dfrac{\partial v_1}{\partial z}+(\delta-\mathrm{i}\,g)v_1+\kappa u_1+Cv_2=0 \\ \mathrm{i}\dfrac{\partial u_2}{\partial z}+(\delta-\mathrm{i}\,g)u_2+\kappa v_2+Cu_1=0 \\ -\mathrm{i}\dfrac{\partial v_2}{\partial z}+(\delta-\mathrm{i}\,g)v_2+\kappa u_2+Cv_1=0 \end{cases}, \tag{1}$$

* This work has been supported by the National Natural Science Foundation of China (No.10704043), and the Natural Science Foundation of Zhejiang Province (No.Y1110078).

** E-mail: liqiliang2@yahoo.com.cn

where u_m and v_m are the envelope functions of the forward and backward traveling waves, δ is frequency detuning from the Bragg frequency, g is gain coeficient, z and τ are space and time coordinates, κ is coupling coefficient between the forward and backward waves, and C is coupling coeficient of the two gratings. We could obtain the analytic solution of Eq.(1) with the boundary conditions of $u_2(0)=v_1(l)=v_2(l)=0$ and $u_1(0)=1$.The refiection coeficient of core 1 is given by

$$r_1=\frac{v_1(0)}{u_1(0)}=\frac{1}{2}\left[\frac{\mathrm{i}\,k\tan(q_1L)}{q_1-\mathrm{i}(\delta+C-\mathrm{i}\,g)\tan(q_1L)}+\frac{\mathrm{i}\,k\tan(q_2L)}{q_2-\mathrm{i}(\delta-C-\mathrm{i}\,g)\tan(q_2L)}\right], \tag{2}$$

where $q_1=\pm\sqrt{(\delta+C-\mathrm{i}g)^2-\kappa^2}$ and $q_2=\pm\sqrt{(\delta-C-\mathrm{i}g)^2-\kappa^2}$ are the characteristic roots of Eq.(1), and L is the FBGC length. The refiectivities and transmittivities of core 1 and core 2 are defined as

$$R_1=|r_1|^2=\left|\frac{v_1(0)}{u_1(0)}\right|^2,\ R_2=|r_2|^2=\left|\frac{v_2(0)}{u_1(0)}\right|^2,$$
$$T_1=|t_1|^2=\left|\frac{u_1(L)}{u_1(0)}\right|^2,\ T_2=|t_2|^2=\left|\frac{u_2(L)}{u_1(0)}\right|^2. \tag{3}$$

From the above equations, the frequency-dependent R and T show the filter characteristics of an FBGC. For q_1, if the frequency detuning δ of the incident light satisfies $(\delta+C)^2<\kappa^2$, q_1 becomes purely imaginary. Most of the incident light is refiected in that range, so grating does not support propagating wave. It is also called the stop band or photonic bandgap. For q_2, if δ satisfies $(\delta-C)^2\leqslant\kappa^2$, the grating does not support propagating wave. By introducing gain in the fiber cores, signal pulse is amplified, and the wave number is changed.

Firstly, we study the influence of gain on the reflectivity and transmittivity of active FBGC. The parameters of FBGC are shown as follows: L=1 cm, κ=3 cm^{-1} and C=1.2 cm^{-1}.

Figs.1 and 2 show the reflectivity and transmittivity of FBGC under different detunings without gain (gL=0) and with gain (gL=0.2). We notice that for all FBGCs, both the reflectivity and the transmittivity are symmetric about detuning. The reflectivity is close to zero when the wavelength is far from bandgap, and it varies rapidly with detuning when it is close to the bandgap. The maximum transmittivity of core 2 may happen when $\delta=\pm5$ cm^{-1}, and the transmittivity of core 1 is zero, so all the power is transferred into core 2. In the bandgap, the transmittivity decreases while the reflectivity increases. When detuning is zero, the refiectivity of core 1 is maximum while the transmittivities of two cores are close to zero. Comparing Fig.1 with Fig.2, we know that the finite gain has no significant influence on the symmetry, while the reflectivity and transmittivity are increased when the gain exists. The transmittivity varies more rapidly with detuning when the wavelength is close to the bandgap. At the bandgap edge, the two peaks of transmittivity in core 1 increase rapidly. So does the transmittivity in core 2.

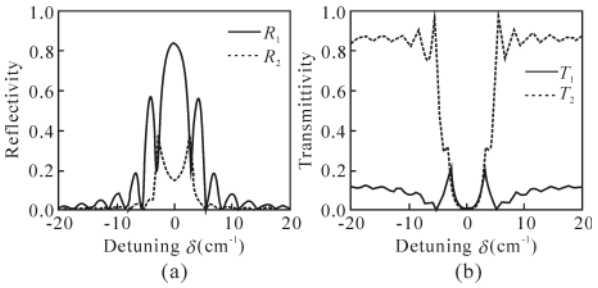

Fig.1 Variations of (a) reflectivity and (b) transmittivity with δ when gL=0

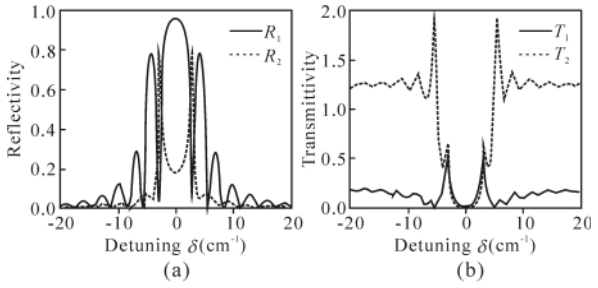

Fig.2 Variations of (a) reflectivity and (b) transmittivity with δ when gL= 0.2

Secondly, we study the induced dispersion of FBGC. In optical fibers, grating-induced dispersion is dominant among all sources responsible for dispersion[1]. The dispersion parameter of an FBGC is given by

$$\beta_2^g=\frac{\mathrm{d}^2q}{\mathrm{d}\omega^2}=-\left(\frac{1}{v_g}\right)^2\frac{\mathrm{d}^2q}{\mathrm{d}\delta^2}=-\left(\frac{1}{v_g}\right)^2\frac{\mathrm{sgn}(\delta+C)\kappa^2}{\{\mathrm{Re}[(\delta+C-\mathrm{i}\,g)^2-\kappa^2]\}^{2/3}}. \tag{4}$$

Because Eq.(1) has two characteristic roots, there are two different second-order dispersions. Fig.3 shows how β_2^g varies with δ for three FBGCs when κ is in the range from 1 cm^{-1} to 10 cm^{-1}.The dispersion parameter of an FBGC β_2^g exceeds that of a uniform fiber β_2 by a large factor. When λ=1.55 μm, $|\beta_2|$ is about 20 ps^2/km, whereas $|\beta_2^g|$ can exceed 10^8 ps^2/km. β_2^g is anomalous on the shorter wavelength side of the stop band, whereas β_2 for fibers becomes anomalous for the wavelength longer than the zero-dispersion wavelength. The distribution of β_2^g of FBG is antisymmetric about $\delta=0$, while when it

comes to FBGC, the symmetry is destroyed due to the coupling coefficient C. β_2^g of FBG changes sign on the two sides of $\delta = 0$, where the wavelength is Bragg wavelength, while β_2^g of FBGC changes sign when $\delta \pm C = 0$, but the wavelength is not Bragg wavelength. Thus, a controllable dispersion can be obtained by changing the wavelength or frequency of input light.

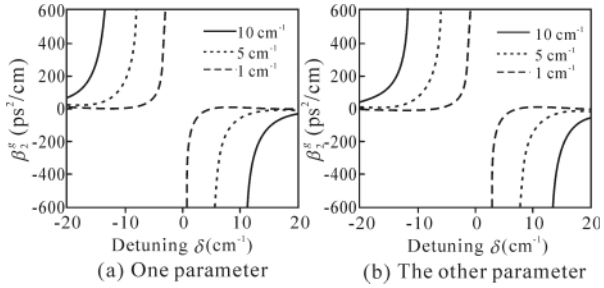

Fig.3 Two different second-order dispersion parameters as a function of δ for several values of κ

Finally, we study the influence of gain on the time delay of active FBGC. The group delay and dispersion of the refiected light can be determined by the phase of the amplitude reflection coefficient r in Eq.(3)[14]. If we write the reflection coefficient r as $r=|r|e^{i\theta_r}$, where θ_r is the phase of r, the delay time of an FBGC is

$$\tau = \frac{d\theta_r}{d\omega} = -\frac{\lambda^2}{2\pi c}\frac{d\theta_r}{d\lambda} \quad . \tag{5}$$

τ is usually given with unit of picoseconds. Denote the delay time for light reflected from core 1 and core 2 as τ_{R1} and τ_{R2}, respectively. The group delay includes time delay $\tau > 0$ and time advancement $\tau < 0$ of the incident pulse after being reflected at the input plane z=0 of the grating. Fast light occurs when $\tau < 0$ and slow light occurs when $\tau > 0$. The parameters of FBGC are L=1 cm, κ=3 cm^{-1} and C=1.2 cm^{-1}. Fig.4 shows the time delays of reflected light in core 1and core 2 as a function of detuning δ when gain is 0, and Fig.5 shows the time delays of reflected light as a function of detuning δ

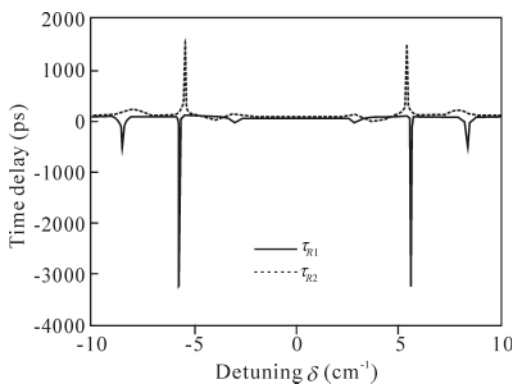

Fig.4 Variation of time delay with δ when g=0

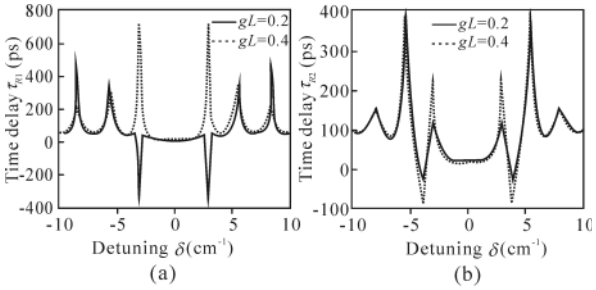

Fig.5 Variation of time delay with δ for different gL values in (a) core 1 and (b) core 2

when gL=0.2 and gL=0.4.

As shown in Fig. 4, the time delay of FBGC is symmetric about detuning. When the wavelength of input light is detuned far from the bandgap, traveling wave has a stable delay which is about 50 ps, and when the wavelength is close to the bandgap, delay varies rapidly with detuning. After introducing gain, the delay is changed completely as shown in Fig.5. The two peaks of delay in core 1 appear when $\delta = \pm 5$ cm^{-1}, and the maximum delay of the reflected light is about 3200 ps, so the pulse in active FBGC is in the fast light range. The magnitude of delay decreases when gain gL=0.2 is introduced. The time delay $\tau < 0$ when $\delta = \pm 2.9$ cm^{-1}, and the pulse is in the fast light regime. And the time delay $\tau > 0$ when $\delta = \pm 5.62$ cm^{-1} and $\delta = \pm 8.37$ cm^{-1}, and the pulse in active FBGC is in the slow light regime. When gain gL=0.4 is introduced, the time delay $\tau > 0$ when $\delta = \pm 2.9$ cm^{-1}, $\delta = \pm 5.62$ cm^{-1}, and $\delta = \pm 8.37$ cm^{-1}, and the pulse in active FBGC is in the slow light regime. The influence of gain on time delay of core 2 only occurs when the wavelength is close to the bandgap, and there is no significant influence when the wavelength is far from bandgap, as shown in Fig.5(b). Thus, a controllable time delay can be obtained by changing the wavelength or frequency of input light.

The time delay and reflectivity spectrum may be changed when the pump power is changed and other parameters are constant. The parameters of FBGC are L=1 cm, κ=3 cm^{-1} and C=1.2 cm^{-1}.

Fig.6 shows how delay and reflectivity vary with g for different detunings, where the detuning is 2.9 cm^{-1} and 5.6 cm^{-1}, respectively. Define the gain point where time delay is 0 as the threshold of gain, written as gL_{th}. When δ=2.9 cm^{-1}, the delay and the reflectivity are shown in Fig.6 (a), where gL_{th}=0.29. When the gain is below gL_{th}, as the gain is increased, the delay and reflectivity first decrease, and then increase. Contrarily, when the gain is above gL_{th}, as the gain is increased, the delay and reflectivity first increase, and then decrease. Correspondingly, at the transition of $gL = gL_{th}$, the group delay τ changes from fast light (for $gL < gL_{th}$) to slow light (for $gL > gL_{th}$). When $\delta = 5.6$ cm^{-1}, gL_{th} decreases to 0.025.

The time delay increases rapidly when gL increases from 0 to $2gL_{th}$, and then decreases as the gain is increased and approaches 50 ps. However, the reflectivity increases as the gain is increased. Thus, a controllable time delay can be obtained by changing the gain.

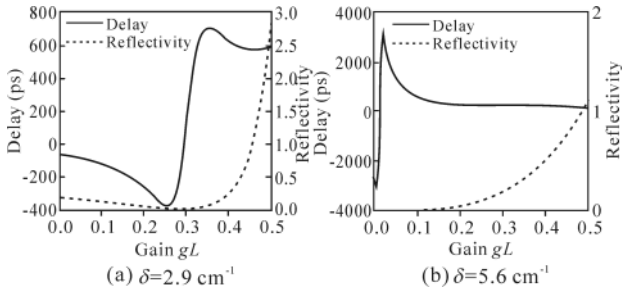

Fig.6 Variation of time delay with gL when δ is (a) 2.9 cm^{-1} and (b) 5.6 cm^{-1}

In conclusion, we theoretically show that tunable delay can be achieved in active FBGC by changing the gain or frequency. The reflectivity of active FBGC in the stop band approaches 100% which is larger than that of uniform FBGC, and the transmittivity increases at both edges of the stop band. The dispersion parameter of FBG is antisymmetric about detuning, while when it comes to FBGC, the symmetry is destroyed due to the coupling coefficient. The time delay of FBGC is symmetric about the detuning, and the magnitude and position of time delay both change when the gain is introduced. Different time delays can be obtained by changing the wavelength or frequency of input light at different gain levels. Meanwhile, delay and reflectivity vary with gain coefficient for different detunings. The results show that different detunings and gain coefficients can result in various time delays, and thus tunable time delay could be achieved by varying signal frequency or gain coefficient. We believe that the tunable time delay, slow light and multi-port characteristics of active FBGC will have important applications in all-optical router, optical buffer, signal processing and optical computing.

References

[1] G. P. Agrawal, Applications of Nonlinear Fiber Optics, Academic Press, San Diego, 97 (2001).

[2] LUO Bin-bin, ZHAO Ming-fu, ZHOU Xiao-jun, HUANG De-yi, WANG Shao-fei and SHI Xiao-hong, Journal of Optoelectronics • Laser **22**, 201 (2011). (in Chinese)

[3] ZOU Xi-hua, PAN Wei, LUO Bin and YAN Lian-shan, Journal of Optoelectronics • Laser **23**, 9 (2012). (in Chinese)

[4] Q. Li, Y. Xie, Y. Zhu, Y. Qi and Z. Zhao, Journal of Lightwave Technology **27**, 2933 (2009).

[5] Y. Okawachi, M. A. Foster, X. Chen, A. C. Turner-Foster, R. Salem, M. Lipson, C. Xu and A. L. Gaeta, Optics Express **16**, 10349 (2008).

[6] M. L. Povinelli, Steven G. Johnson and J. D. Joannopoulos, Optics Express **13**, 7145 (2005).

[7] Y. Peng, K. Qiu, B. Wu and S. Ji, Optik-International Journal for Light and Electron Optics **122**, 881 (2011).

[8] O. V. Belai, E. V. Podivilov and D. A. Shapiro, Optics Communications **266**, 512 (2006).

[9] K. Qian, L. Zhan, H. Li, X. Hu, J. Peng, L. Zhang and Y. Xia, Optics Express **17**, 22217 (2009).

[10] J. T. Mok, C. M. D. Sterke, I. C. M. Littler and B. J. Eggleton, Nature Physics **2**, 775 (2006).

[11] S. Longhi, Physical Review E **72**, 056614 (2005).

[12] H. Shahoei, M. Li and J. Yao, Journal of Lightwave Technology **29**, 1465 (2011).

[13] H. Shahoei and J. Yao, Journal of Lightwave Technology **30**, 1954 (2012).

[14] T. Erdogan, Journal of Lightwave Technology **15**, 1277 (1997).